Open system quantum thermodynamics of time-varying graphs

GIORGIA MINELLO[†] AND ANDREA TORSELLO

Dipartimento di Scienze Ambientali, Informatica e Statistica, Università Ca' Foscari Venezia, Via Torino 155, 30172 Venezia Mestre, Italy
[†]Corresponding author. Email: giorgia.minello@unive.it

AND

EDWIN R. HANCOCK

Department of Computer Science, University of York, Deramore Lane, York YO10 5GH, UK

Edited by: Jesus Gomez-Gardenes

In this article, we present a novel analysis of time-evolving networks, based on a thermodynamic representation of graph structure. We show how to characterize the evolution of time-varying complex networks by relating major structural changes to thermodynamic phase transitions. In particular, we derive expressions for a number of different thermodynamic quantities (specifically energy, entropy and temperature), which we use to describe the evolutionary behaviour of the network system over time. Since in the real world no system is truly closed and interactions with the environment are usually strong, we assume an open nature of the system. We adopt the Schrödinger picture as the dynamical representation of the quantum system over time. First, we compute the network entropy using a recent quantum mechanical representation of graph structure, connecting the graph Laplacian to a density operator. Then, we assume the system evolves according to the Schrödinger representation, but we allow for decoherence due to the interaction with the environment in a model akin to *Environment-Induced Decoherence*. We simplify the model by separating its dynamics into (a) an unknown time-dependent unitary evolution plus (b) an observation/interaction process, and this is the sole cause of the changes in the eigenvalues of the density matrix of the system. This allows us to obtain a measure of energy exchange with the environment through the estimation of the hidden time-varying Hamiltonian responsible for the unitary part of the evolution. Using the thermodynamic relationship between changes in energy, entropy, pressure and volume, we recover the thermodynamic temperature. We assess the utility of the method on real-world time-varying networks representing complex systems in the financial and biological domains. We also compare and contrast the different characterizations provided by the thermodynamic variables (energy, entropy, temperature and pressure). The study shows that the estimation of the time-varying energy operator strongly characterizes different states of a time-evolving system and successfully detects critical events occurring during network evolution.

Keywords: graph; thermodynamics.

1. Introduction

The problem of identifying an effective and succinct characterization of complex network structure has been the ongoing focus of interest in network analysis for several decades [1–3]. Initially, efforts focused around a static view of network structure and on developing ways to describe networks through identifying salient substructures, such as communities, hubs or clusters [4–6]. In these cases the resulting representation is defined by the connectivity structure [7], and this approach has proved effective for

problems of both clustering and classification [8, 9]. Recently, on the other hand, dynamical network analysis has attracted more attention. In particular, the analysis of the processes underlying network evolution and the detailed mechanisms involved have both acquired an increasingly crucial role in network science. However, capturing the large-scale properties of a time-evolving structure has proven to be an extremely challenging problem. For searching for structural changes in temporal networks, the classic methods described in the literature usually adopt tools from statistics. For instance, in [10], statistical process control techniques are used in order to detect changes in social networks. Methods relying on machine learning are also common, and these include [11]. Here the authors formalize the problem of detecting change-points in large-scale evolving structures using an online probabilistic learning framework. Alternative approaches employ statistics and image analysis techniques to detect anomalies in graph time series. For example, in [12] the authors introduce a theory of scan statistics on graphs.

From the perspectives of both static and dynamic network analysis, many researchers have recognized that drawing on ideas from fields such as physics, may yield promising results. For instance, the use of analogies based on statistical mechanics [13–18], thermodynamics [19–21] as well as quantum information [7, 22, 23] provides an excellent framework for describing complex time-evolving systems. Among these the approaches based on thermodynamic analogies, relating the behaviour of microscopic particles to the macroscopic properties of a system [16, 17, 24], have proved remarkably successful. For example, the heat bath analogy from thermodynamics described in [25] allows us to define physical measures of communicability and balance in networks.

When the network is described by a partition function, thermodynamic quantities, such as entropy, energy and temperature can be straightforwardly derived from it [26]. Usually in these cases the Hamiltonian is obtained from the adjacency matrix or Laplacian matrix of the network and their eigenvalues. The choice of partition function governs how the different energy levels are populated and thus the details of how the thermodynamic quantities characterizing a network depend on temperature and the distribution of energy levels. This means that the choice of partition function also determines the domain of applicability of the developed graph characterization.

For instance, in [20] the authors use the Maxwell–Boltzmann partition function to describe a system in thermal equilibrium with a heat bath and show how the partition function can be computed from a characteristic matrix polynomial.

By contrast, in [27] the Bose–Einstein partition function models a Bose gas over a network. In this case, the process of Bose–Einstein condensation provides deep insights into low temperature network behaviour including the formation of a condensate through the coalescences of particles into the lowest energy states.

In network analysis and especially for those methods based on statistical physics analogies, most approaches adopted to study complex structures are based on concepts from spectral graph theory [28]. For instance, in the heat bath analogy utilized to characterize networks, the energy states of a network are captured using the eigenvalues of the matrix representation of the network [29]. Here, in particular, global network characteristics, including the entropy, can be computed by using the Maxwell–Boltzmann partition function. By contrast, in [30, 31] energy states are occupied according to either Bose–Einstein or Fermi–Dirac statistics. For time-evolving structures, thermodynamic approaches and spectral analysis have also proved to be extremely useful as tools for characterizing dynamic networks. For instance the von Neumann entropy of a network was firstly introduced by Braunstein [22] and analysed further in a number of subsequent works [7, 23]. The idea underpinning this measure is that the combinatorial graph Laplacian can be interpreted as the density matrix of a quantum system. In [21], the spectrum of the normalized Laplacian matrix is used to define the microstates of a complex system, and the associated microstate occupation probabilities are used to define the thermodynamic entropy of the network. Additionally, the

authors show how to compute thermodynamic variables in terms of node degree statistics. Similarly, in [32] the authors investigate the variation of entropy in time-evolving networks and show how global modifications of network structure are determined by correlations in the changes in joint degree statistics for those pairs of nodes connected by edges. Thus, thermodynamic approaches can not only be used to characterize networks utilizing classical measures, such as entropy or energy, but can also be used to develop new measures of network complexity. For instance in [19], for the case of graph representation of complex networks, a flow complexity measure is presented and a thermodynamic characterization is developed based on the variation of local histories over graphs.

1.1 *Overview*

Recently, the literature has witnessed a large volume of work aimed at understanding the evolution of time-varying networks by means of analogies and formal similarities with thermodynamics and quantum information. However, most attempts construct their analysis around a given Hamiltonian, *de facto* assuming a complete representation of the system to be studied is at hand.

In this work we look at a different and less studied scenario, where the network is only a partial component of a larger system and its evolution is affected by the interaction with the larger environment.

Here, following [33] we define the environment as any set of degrees of freedom that are coupled to the system of interest, and which we can therefore monitor and become entangled with its states. In an approach akin to *Environment-Induced Decoherence* [33], we model the system interaction with the environment as an open system subject to internal and external potentials (unitary component), as well as the monitoring effect of the environment (entropic component).

Following a classic renormalization approach, we assume that these forces act at a different time-scale, so that they can be effectively approximated by a (time-varying) potential term in the Hamiltonian coupled with an observation/interaction process, sole cause of the change in the eigenvalues of the density matrix. The fact that the effects of the environment are unknown, results in an unknown potential and thus an unknown effective Hamiltonian, which we need to estimate from the evolution of the network. This results in an inverse-problem formulation from the observed dynamics to estimate the thermodynamic quantities. With this formulation to hand, we aim at analysing, comparing and contrasting the characterization quality of the obtained thermodynamics measures. The goal is to see whether major variations in the thermodynamic-variables are linked with fundamental topological changes and key events in the evolution of the system.

In our approach, the graph Laplacian at each time epoch is viewed as a quantum mixed state undergoing free evolution through the Schrödinger equation under an unknown time-dependent Hamiltonian. Here, the free evolution of a quantum system means the time evolution of a system generated by some Hamiltonian. In particular, the Hamiltonian represents the change in potential energy due to external factors. Entropy and energy change with time as a result of direct interaction between the system and its environment. From the observed evolution of the network (i.e. the system), we estimate the Hamiltonian together with the energy exchange with the environment at each time epoch, as well as the variation in entropy of the underlying structure (system). Finally, from these variations we derive the actual thermodynamic variables of the evolving network system, including the energy and temperature.

The resulting characterization is utilized to represent the evolution of a number of real-world time-varying networks. These include (a) the price correlation of selected stocks in the New York Stock Exchange (NYSE) [34], (b) the gene expression of the life cycle of the Fruit Fly (*Drosophila melanogaster*) [35, 36] and (c) a further financial network, United States Stock Market (USSM). First, we develop the framework for networks with a fixed number of nodes. This is a quite common feature

of networks used to abstract systems with a known set of components or states. Then, we show how the formulation can be extended to take into account variation in network size, under the assumption of a fixed pressure which becomes a mixing parameter balancing the effect of changes in energy and network size.

The remainder of the article is organized as follows. In Section 2, we present the mathematical and thermodynamic background. In addition, we provide a detailed development of how we compute the thermodynamics variables under the fixed-volume assumption. In Section 3, we apply the resulting thermodynamic representation to a number of real-world time-varying networks. In Section 4, we generalized the analysis to size-changing networks, and finally in Section 5 we present our conclusions.

2. Quantum thermodynamics of the network

Let $G(V, E)$ be an undirected graph with node set V and edges set $E \subseteq V \times V$ and let $A = a_{ij}$ be the adjacency matrix, where

$$a_{ij} = \begin{cases} 1, & (v_i, v_j) \in E, \\ 0, & \text{otherwise.} \end{cases}$$

The degree d of a node is the number of edges incident to the node and it can be represented through the degree matrix $D = (d_{ij})$ which is a diagonal matrix with $d_{ii} = \sum_i a_{ij}$. The graph Laplacian is then defined as $L = D - A$, and it can be interpreted as a combinatorial analogue of the discrete Laplace-Beltrami operator. The normalized Laplacian matrix $\tilde{L}$ is defined as

$$\tilde{L} = D^{-1/2}(D - A)D^{-1/2}. \tag{2.1}$$

In standard quantum mechanics, the state of a quantum mechanical system associated to the n-dimensional Hilbert space $\mathsf{H} \cong \mathbb{C}^n$ is identified by a $n \times n$ positive semidefinite Hermitian matrix, with $\text{Tr}(\rho) = 1$, the *density matrix*. The *density operator* is introduced in quantum mechanics to describe a system whose state is an ensemble of pure quantum states $|\psi_i\rangle$, each with probability p_i. In other words, every density matrix can be written as a weighted sum of pure states, with real non-negative weights summing up to 1.

$$\rho = \sum_i p_i |\psi_i\rangle \langle \psi_i|. \tag{2.2}$$

There are different ways to associate graphs to specific states or dynamics, for example, graph-states [37, 38] or spin networks [39–41]. However, here we opt for another approach, the mapping between discrete Laplacian and quantum states, firstly introduced by Braunstein *et al.* [22] (see also [42]). In the first place, it is easy to observe how the normalized Laplacian matrix, scaled by the number of vertices in the graph, has the characteristic features of a quantum mechanical density matrix: it is a positive semidefinite unit trace matrix, which actually provides a link to quantum states. In [23], Passerini and Severini suggest how the normalized Laplacian can be also seen as a density matrix in a quantum system representing a quantum superposition of the transition steps of quantum walk over the graph. Furthermore, the normalized Laplacian may be interpreted as a mixture of pure states (i.e. a convex combination of rank-1 operators), more precisely a uniformly random mixture of pure states in the vertex-space, where each state in the mixture corresponds to a single edge of the graph [43]. In this way, we can associate with any graph G a specific mixed quantum state [42].

The Shannon entropy measures the uncertainty associated with a classical probability distribution. However, if we replace probability distributions with density operators, we can generalize the definition of the Shannon entropy to quantum states (actually described in a similar fashion), obtaining in fact the entropy of a quantum state. More to the point, the *von Neumann entropy* [44] or *quantum entropy H_N* of a mixed state is defined in terms of the trace and logarithm of the density operator ρ

$$H_N = -\operatorname{Tr}(\rho \log \rho) = -\sum_i \xi_i \ln \xi_i, \tag{2.3}$$

where $\xi_1, \dots, \xi_n$ are the eigenvalues of ρ. In this sense, the quantum entropy is related to the distinguishability of the states, that is, the amount of information that can be extracted from an observation of the mixed state. In [22], Braunstein *et al.* introduce the von Neumann entropy as a quantitative measure of mixedness of the density matrix ρ. This definition in turn is based on the mapping between quantum states and the combinatorial graph Laplacian, as discussed above. Many detailed studies followed this work [1, 7, 23, 43, 45–47], but one in particular deserves more attention. Precisely, Passerini and Severini in [23] investigated the use of the normalized Laplacian as a density operator to define the current state of the network, thus allowing the network entropy to be derived using the quantum mechanical definition of the von Neumann entropy

$$S_{VN} = -\sum_{i=1}^{|V|} \frac{\tilde{\lambda}_i}{|V|} \ln \frac{\tilde{\lambda}_i}{|V|}, \tag{2.4}$$

where $\tilde{\lambda}_1, \dots, \tilde{\lambda}_n$ are the eigenvalues of $\tilde{L}$ and $|V|$ defines the number of vertices. In the same work, they provide an interpretation of this quantity as a measure of regularity for graphs. The resulting intuition is thus that we can somehow measure the complexity of a graph through the von Neumann entropy. Nevertheless, the interpretation of this spectral measure, in terms of structural patterns, is as yet unclear, as pointed-out in [48]. Specifically, the ability to distinguish certain structural patterns is strictly influenced by the topology of the underlying graph. In other words, measures of this type are extremely sensitive to the structural properties of graphs, such as symmetries [49]. Consequently, we adopt this quantum approach in the analysis of network, not so much because we believe the system or its evolution to be quantum in nature, but due to the observed sensitivity to structural changes of these quantum structure-probing mechanisms.

The *continuous-time quantum walk* is the quantum counterpart of the continuous-time random walk, and it is similarly defined as a dynamical process over the vertices of the graph [50]. Here the classical state vector is replaced by a vector of complex amplitudes over V, and a general state of the walk is a complex linear combination of the basis states $|v\rangle, v \in V$, such that the state of the walk at time t is defined as

$$|\psi_t\rangle = \sum_{u \in V} \alpha_u(t) |u\rangle, \tag{2.5}$$

where the amplitude $\alpha_u(t) \in \mathbb{C}$ and $|\psi_t\rangle \in \mathbb{C}^{|V|}$ are both complex. Moreover, we have that $\alpha_u(t)\alpha_u^*(t)$ gives the probability that at time t the walker is at the vertex u, and thus $\sum_{u \in V} \alpha_u(t)\alpha_u^*(t) = 1$ and $\alpha_u(t)\alpha_u^*(t) \in [0, 1]$, for all $u \in V, t \in \mathbb{R}^+$.

The evolution of the walk is then given by the Schrödinger equation, where we denote the (possibly time-dependent) Hamiltonian as $\mathscr{H}$.

$$\frac{\partial}{\partial t} |\psi_t\rangle = -i\mathscr{H} |\psi_t\rangle. \tag{2.6}$$

Time-dependent Hamiltonian, within the context of the Schrödinger equation, means that there is an external interaction of the system which manifests itself by a time-dependent potential term. In general, the Schrödinger's equation must be solved for the joint state describing system and environment together. However, for certain Hamiltonians and initial quantum states of the environment, the open system's dynamics can be well described by an effective (possibly time-dependent) potential term in the Hamiltonian, to some good approximation.

Here, we assume that the dynamics of the network is governed by the Schrödinger equation together with an interaction with the external world, which acts as an observer thus affecting the entropy and exchanging energy with the system. We model the effect of this interaction as a two component process: (a) the first component neither changes the thermodynamic variables nor causes any variation in the entropy; this can be seen as an external potential that can be absorbed into the (unknown) Hamiltonian thus developing its time-dependency an (b) the second component is modelled as an observation-like process causing changes in entropy in the network and thus a corresponding exchange in energy with the environment.

We recall that in quantum mechanics, for every physical observable there is an associated operator. Roughly speaking, a physical observable is anything that can be measured. The energy is thus defined in terms of the energy operator. To measure the energy exchange we need to recover the potential term expressed by the unknown Hamiltonian. In fact, the Hamiltonian acts as an energy operator, so that the expected energy of a generic state ρ can be computed as $\text{Tr}(\mathscr{H}\rho)$. This results in the following expression for the change in energy between state ρ_t and ρ_{t+1}

$$dU = \text{Tr}(\mathscr{H}_{t+1}\rho_{t+1}) - \text{Tr}(\mathscr{H}_t\rho_t). \tag{2.7}$$

We estimate the Hamiltonian $\mathscr{H}_t$ as the one that minimizes the exchange of energy through the interaction with the external environment. Intuitively this derives from the observation that free evolution under the Schrödinger equation changes neither the entropy nor the energy, and that any such change has to derive from the interaction with the external environment. The reason for estimating the interaction as the one which minimizes the exchange of energy is that a more energetic interaction should be less probable in a statistical mechanic sense. To this end, we adopt a simplified model where the interaction intervenes at the end of the free evolution. This means that we model the complex interactions as an evolution under the Schrödinger equation between times t and $t + 1$, followed by an instantaneous interaction with the external world at time $t + 1$ during which all the energy and entropy exchange occurs.

Approximating the Hamiltonian with a piecewise constant operator, we can use the time-invariant Schrödinger equation to estimate the constant value of the Hamiltonian between time epochs t and $t + 1$ through the use of the unitary transformation

$$\mathscr{U}(s,t) = \exp(-i\hat{\mathscr{H}}_t(s - t)) \tag{2.8}$$

which provides a solution for the evolution induced by the Schrödinger equation. Here, $\hat{\mathscr{H}}_t$ denotes the approximate Hamiltonian that we estimate from the evolution, and $s \in [t; t + 1)$ is any time within the

unit time interval commencing at t. This results in

$$\hat{\rho}_{t+1} = \exp(-i\hat{\mathcal{H}}_t)\rho_t \exp(i\hat{\mathcal{H}}_t), \tag{2.9}$$

where $\hat{\rho}_{t+1}$ is the density at time $t + 1$ just prior to the instantaneous energy-exchanging process.

The exchange of energy in the interaction is then

$$\begin{aligned}
\Delta U_t &= \mathrm{Tr}(\hat{\mathcal{H}}_t \rho_{t+1}) - \mathrm{Tr}(\hat{\mathcal{H}}_t \hat{\rho}_{t+1}) \\
&= \mathrm{Tr}\left(\hat{\mathcal{H}}_t\big(\rho_{t+1} - \exp(-i\hat{\mathcal{H}}_t)\rho_t \exp(i\hat{\mathcal{H}}_t)\big)\right)
\end{aligned} \tag{2.10}$$

from which we can estimate the Hamiltonian as the operator that minimizes this quantity.

Let $\rho_t = \Phi_t \Lambda_t \Phi_t^T$ be the spectral decomposition of the state of the network at time t, equation (2.10) can be solved by noting that the unitary evolution implicit in the Schrödinger equation does not change the eigenvalues of the density matrix, but only rotates its eigenvectors. Hence, under the assumed two component interaction model, we allow the unitary component to be the one that aligns the eigenvectors in such a way that the absolute difference between the corresponding eigenvalues is minimized. Thus the second model component, that is, the entropy-changing observation process, only needs to change the relative population of each state in the ensemble. As a consequence, the minimum energy exchange intervenes when the interaction changes the eigenvalues of the density matrices, and with them the entropy, but does not change the corresponding eigenspaces. In other words, the Hamiltonian is the cause of the eigenvector rotation, while the interaction with the environment causes only the rotation of the eigenvalues. Under this assumption, the Hamiltonian can be recovered from the aligning rotation $\mathcal{U} = \Phi_{t+1} \Phi_t^T$ recalling that $\mathcal{U} = \exp(-i\hat{\mathcal{H}}_t)$. This results in

$$\hat{\mathcal{H}}_t \approx i \log(\Phi_{t+1} \Phi_t^T). \tag{2.11}$$

It is worth noting that we have computed a lower bound of the Hamiltonian, since we cannot observe components on the null spaces of ρ.

The final change in internal energy is then

$$dU_t = Tr(\hat{\mathcal{H}}_{t+1}^{-}\rho_{t+1}) - Tr(\hat{\mathcal{H}}_t^{+}\rho_t) = Tr(\hat{\mathcal{H}}_{t+\frac{1}{2}}(\rho_{t+1} - \rho_t)), \tag{2.12}$$

where $\hat{\mathcal{H}}_{t+1}^{-}$ and $\hat{\mathcal{H}}_t^{+}$ are respectively the left and right limit of the top and bottom of the interval. Due to the piecewise-constant approximation we have

$$\hat{\mathcal{H}}_{t+1}^{-} = \hat{\mathcal{H}}_t^{+} = \hat{\mathcal{H}}_{t+\frac{1}{2}}. \tag{2.13}$$

In the general time-varying case, the evolution operator can be expressed as

$$\mathcal{U}(s,t) = \exp(-i\Omega(s,t)), \tag{2.14}$$

where $\Omega(s, t)$ can be obtained from the Hamiltonian through a Magnus series [51]. To estimate the exchange in energy, we compute the variation in energy from ρ_t to $\hat{\rho}_{t+1}$ as

$$
\begin{aligned}
dU &= \int_t^{t+1} \mathrm{Tr}\left(\mathscr{H}_s \rho_s\right)\, ds \\
&= \int_t^{t+1} \mathrm{Tr}\left(\mathscr{H}_s \mathscr{U}(s, t)\, \rho_t\, \mathscr{U}^\dagger(s, t)\right)\, ds \\
&= \int_t^{t+1} \mathrm{Tr}\left(i \frac{d\,\mathscr{U}(s, t)}{ds}\, \rho_t\, \mathscr{U}^\dagger(s, t)\right)\, ds \\
&= \int_t^{t+1} \mathrm{Tr}\left(\mathscr{U}(s, t) \left(\frac{I - \exp(i\, \mathrm{ad}_\Omega)}{-i\, \mathrm{ad}_\Omega}\right) \Omega'(s, t)\, \rho_t\, \mathscr{U}^\dagger(s, t)\right)\, ds \\
&= \mathrm{Tr}\left(\int_t^{t+1} \mathscr{U}(s, t) \left(\frac{I - \exp(i\, \mathrm{ad}_\Omega)}{-i\, \mathrm{ad}_\Omega}\right) \Omega'(s, t)\, ds\, \rho_t\right) \\
&= \mathrm{Tr}\left(\Omega(t+1, t)\, \rho_t\right),
\end{aligned} \tag{2.15}
$$

where the derivative of the exponential $\mathscr{U}(s, t) = \exp(-i\Omega(s, t))$ is

$$
\frac{d\,\mathscr{U}(s, t)}{ds} = \mathscr{U}(s, t) \left(\frac{I - \exp(i\, \mathrm{ad}_\Omega)}{-i\, \mathrm{ad}_\Omega}\right) \Omega'(s, t). \tag{2.16}
$$

Here ad_Ω is the adjoint operator [52] and $\Omega'(s, t)$ is the derivative of $\Omega(s, t)$.

As a consequence, the exchange in energy is

$$
dU_t = Tr(\Omega(t+1, t)\rho_{t+1}) - Tr(\Omega(t+1, t)\rho_t). \tag{2.17}
$$

This means that the unitary operator minimizing the exchange in energy is still

$$
\mathscr{U} \approx \Phi_{t+1} \Phi_t^T \tag{2.18}
$$

and that $\hat{\mathscr{H}} = i\log(\mathscr{U})$ can be used as an effective 'mean energy' operator to compute the energy differences.

With the energy operator to hand, the thermodynamic temperature T can then be recovered through the fundamental thermodynamic relation $dU = TdS - PdV$ but where we assume that the volume is constant, that is, $dV = 0$ (isochoric process). As a result, the temperature T is simply the rate of change of entropy with energy

$$
T = \frac{dU}{dS}. \tag{2.19}
$$

This definition can be applied to evolving complex networks which do not change the number of nodes during their evolution.

3. Experiments and evaluations

In this section, we explore the ability of the thermodynamic formulation to identify global topological changes in structure. In particular, we apply the analysis to three real-world time-evolving networks in order to assess the ability of the thermodynamic formulation to identify important topological transitions in network structure and characterize the overall dynamics of the system. First, we give a brief overview of the three datasets extracted from real-world complex systems, then we discuss the outcomes of the analysis. Wherever possible we make a comparison with similar approaches.

3.1 *Datasets*

Here, we use three data sets. The first and third sets are based on financial data, whereas the second comes from the biological domain.

3.1.1 *Dataset 1—NYSE.* The dataset is extracted from a database consisting of the daily prices of 3799 stocks continuously traded on the New York Stock Exchange (NYSE). To construct the dynamic network, 347 stock with historical data from May 1987 to February 2011 are selected [34]. In order to construct an evolving network, a time window of 28 days is used and it is moved along time to obtain a sequence (from Day 29 to Day 6004); in this way, each temporal window contains a time-series of the daily return stock values over a 28-day period. Trades among the different stocks are represented as a network. For each time window, we compute the cross-correlation coefficients between the time-series for each pair of stock and create connections between them if the absolute value of the correlation coefficient exceeds a threshold. The result is a stock market network which changes over the time, with a fixed number of 347 nodes and varying edge structure for each of trading days.

3.1.2 *Dataset 2—Drosophila.* The dataset comes from the field of developmental biology, and concerns the interactions among genes of *Drosophila melanogaster*—better known as the fruit fly—during its life cycle. The data are sampled at 66 sequential developmental time points. The fruit fly life cycle is divided into four stages, namely (a) the embryonic (samples 1–30), (b) larval (samples 31–40) and (c) pupal (samples 41–58) periods together with (d) the first 30 days of adulthood (samples 59–66). Early embryos are sampled hourly and adults are sampled at multi-day intervals, according to the speed of the morphological changes. To represent these data using a time-evolving network, the following steps are followed [36]. At each developmental point the 588 genes that are known to play an important role in the development of the *Drosophila* are selected. These genes are the nodes of the network, and edges are established based on the microarray gene expression measurements reported in [35]. To make the normalized Laplacian more tractable, any self-loop in the obtained undirected graph has been removed, at each time step. This dataset yields a time-evolving network with a fixed number of 588 nodes, sampled at 66 developmental time points.

3.1.3 *Dataset 3—USSM.* The dataset USSM is extracted from a database of the daily prices of 431 companies in eight different sectors from the New York Stock Exchange and the NASDAQ Stock Market (NASDAQ). Data have been gathered from January 1995 to December 2016. The dataset is arranged to be around 5500 trading days and built similarly to the NYSE dataset, that is, a time window of 28 days is used and moved along time to obtain sequences of the daily return stock values. Then the cross correlation coefficients between each pair of stocks time-series are used to define links. The resulting network is an
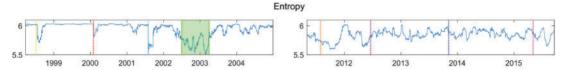
Entropy

FIG. 1. USSM dataset—entropy vs time. Main market crises are highlighted by vertical lines. Left: Russian Financial Crisis—Ruble devaluation (17th August 1998), Dot-com bubble—climax (10th March 2000), September 11 attacks 2001, Downturn of 2002–2003. Right: Stock Markets Fall (August 2011), Greek legislative election (June 2012), United States debt-ceiling crisis (October 2013) and Chinese stock market turbulence 2015.

evolving stock market network where the number of nodes is fixed (equal to 431) but the edge structure is constantly changing.

For the sake of completeness, it should be noted that networks inferred by means of computing time series cross-correlation and thresholding procedures are very sensitive to the chosen parameters. Thresholding generally retains the strongest edges. However, the choice of level of interaction—namely defining if an edge is sufficiently strong to count in a network—actually may affect the properties associated with the network. Unfortunately, the inference of stable network structures from time series data is still an open issue which is still an active area of research in the literature [53].

3.2 *Experiments*

We aim at analysing how the thermodynamic variables describe network evolution and specifically if they can detect critical events as the system develops (e.g. financial crises or crashes in the stock market and morphological changes during the fruit fly life cycle). To conduct our analysis, at each time interval, we computed the normalized Laplacian of the network which we used to estimate the Hamiltonian. Then entropy and energy state variables have been calculated using equations 2.4 and 2.7, respectively. However, it should be noted that we deal with open systems, which do not evolve towards an equilibrium. Therefore, we do not expect to observe any conservation in energy or a constant increase in entropy either. On the other hand, we expect to observe some pattern of variation in these quantities, as evidence of topological dynamics or reactions of the networks to their environment.

An illustrative example is given by Fig. 1, which is composed of two panels representing the entropy vs time, in two different time windows (1998–2004 and 2011–2015). From the two plots, it is clear that the von Neumann entropy allows us to interpret the network behaviour. For instance, by comparing the two panels, it is clear that in the left-hand one (1998–2004) the crises are characterized by sudden drops in entropy. On the other hand, in the right-hand plot (2011–2015) the entropy is unstable. This suggests that the underlying nature of the financial markets has changed with time (e.g. by the introduction of high-frequency automatic trading). In particular, as suggested by various authors [23, 48, 54], the von Neumann entropy provides an insight into the network complexity. However, to date, we have no direct link or explicit map between entropy values and the structural changes occurring in the network. Nevertheless, we can observe the effect of network alterations in terms of their impact on the temporal tendencies of the entropy.

We commence our study by analysing variations in thermodynamic quantities, specifically entropy and energy, and next, we will examine the relationships between them. In Fig. 2, we show their time series for the US Stock Market data. Both quantities detect financial and political factors, which have influenced the structure of the trading network. However, the entropy variation sometimes appears somewhat noisier than the energy, probably because it is more susceptible even to slight structural mutations. In Fig. 3,
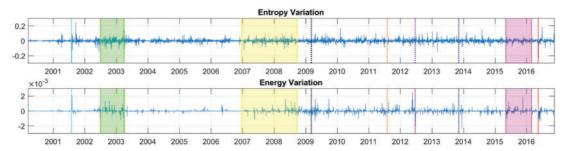
FIG. 2. USSM dataset—entropy and energy variation vs time, respectively top and bottom chart. The vertical coloured lines mark some important events for the trade market: September 11 attacks, Downturn of 2002–2003, Financial Crisis of 2007–2008, Dow Jones lowest point (March 2009), Stock Markets Fall (August 2011), Greek legislative election (June 2012), United States debt-ceiling crisis (October 2013), Chinese stock market turbulence 2015 and Brexit Referendum (June 2016).
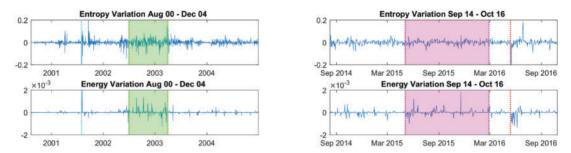

FIG. 3. USSM dataset—entropy and energy variation vs time, respectively top and bottom, details. The vertical coloured lines refer to political and financial affecting the trade market. Left: September 11 attacks, Downturn of 2002–2003. Right: Chinese stock market turbulence 2015–2016 and Brexit Referendum (June 2016).

we study two financial crises in detail, namely the Downturn of 2002–2003 and Chinese stock market turbulence 2015–2016. We observe how crises are well localized in energy dimension but less well so in entropy. Moreover, the entropy variation time series between 2004 and 2006 does not look so stable in comparison to the energy dimension. In fact, during this intermediate period, the energy exchange is small, and this corresponds to a period of prolonged network stability. In other words, energy exchange proves to be effective in characterizing the network state as well as in the estimation of the hidden time-varying Hamiltonian which successfully extracts information concerning the change in network structure.

Now, we investigate the relationship between the previous thermodynamic quantities by studying the network temperature. This variable has been calculated similarly to Eq. 2.19. However, to reduce excessive surges or drops, we performed a Laplace smoothing of the series by adding a constant ε to the denominator, that is, to the entropy variation dS. The individual time-series for the thermodynamic variable shown in Fig. 4 clearly presents many significant fluctuations, most of them corresponding to some realistic major financial crises, for example, the Downturn of 2002–2003, as well as significant influential political events, for example, the Brexit referendum. Another interesting feature in the figure is that, although the network structure becomes particularly unstable after the Financial Crisis of 2007–2008, different crucial events are still detectable. This in turn tells us that this dimension provides the fundamental information to capture the market trend. Unlike the quantum entropy in the graphs domain, which is a well-established topic in the literature, the temperature, specifically its interpretation in terms of
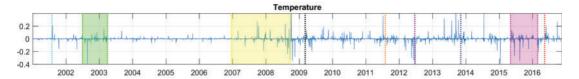
FIG. 4. USSM dataset—temperature vs time. The vertical coloured lines refer to some important events for the trade market: September 11 attacks, Downturn of 2002–2003, Financial Crisis of 2007–2008, Dow Jones lowest point March 2009, August 2011 stock markets fall, Greek legislative election June 2012, United States debt-ceiling crisis October 2013, Chinese stock market turbulence 2015–2016 and Brexit Referendum June 2016.
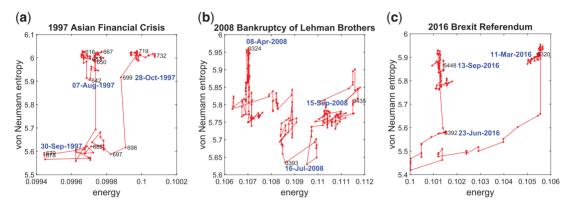

FIG. 5. USSM dataset—trace of the time-evolving stock correlation network in the entropy–energy plane during financial crises. (a) Asian Financial Crisis (July 1997–December 1997); (b) Lehman Brothers Bankruptcy (January 2008–October 2008); and (c) Brexit Referendum (March 2006–September 2016).

network analysis, has not reached a clear formalization yet. Nevertheless, Ye *et al.* in [21] have attempted to provide an insight about the connection between temperature and network behaviour, by defining the thermodynamic variables by means of node degree statistics for nodes connected by edges. In particular, according to their definitions, a low temperature is observed when there are large local variations in edge structure, whereas when there is a significant overall change in the number of edges, the temperature tends to become higher. Moreover, since this observation is based on the von Neumann entropy properties, such insights also apply in our formulation.

Figure 5 shows the trace of the stock market network on the entropy–energy plane during three different financial crises. We show the ordinal number of the days which correspond to significant events in the time series. Those key data points are also highlighted by annotating them with the corresponding date. In the left-hand panel we show (a) the data for the Asian Financial Crisis (days 616 to 732 from July 1997 to December 1997), (b) in the middle panel the Lehman Brothers Bankruptcy (days 3269 to 3479 from January 2008 to October 2008) and (c) in the right-hand panel the Brexit Referendum period (days 5320 to 5450 March 2006 to September 2016). At first sight, it seems that there exists a temporal blocking behaviour in each of the plots. Additionally, we can draw the following conclusions from the three plots:

• For the Asian crisis, the network appears to move from a well-defined phase to another one, passing through a short intermediate transition stage. In fact, the Asian financial crisis began in the summer

of 1997 and spread through many Asian markets during July and August of that year. However, only in October was a recovery plan triggered with the injection of loans from the International Monetary Fund (IMF). This is reflected in the corresponding plot. Preceding the crisis the network was first in a stable state, then a transient period occurs and finally there is the recovery phase. In particular, the entropy dimension collapses concomitantly with the transient state. This means there are no significant interactions within the network. Subsequently there is a return to higher (and normal) entropy values. Moreover, there appears to be a clear distinction between the crisis peak and the preceding and succeeding epochs. On the other hand, for the energy dimension, the period occupied by the actual crisis and the subsequent are well distinguished. Actually, higher energy is related to a greater market volume and this is a clear differentiating factor. It is important to recall that the energy is obtained via the estimation of the Hamiltonian. In other words, the fact that the energy dimension is capable of capturing and distinguishing different temporal blocks or market epochs underlines the effectiveness of the method.

- In a similar way, in the right-hand panel (Brexit) the transition is again correctly captured. Here, when the result of the referendum is known (June 2016), the network undergoes substantial change in structure. Both the entropy and the energy decrease rapidly. Then, the entropy returns to its original range of values after the referendum result. Indeed, once the crisis is over, the pattern of trading relations is re-established and thus the entropy increases. This also means that the network returns to its normal state, even if the energy tends to remain low—as if the referendum still has residual effects on the volume of market trades.

- The middle plot (Lehmann Brothers) is probably the most chaotic, but in practice it precisely captures the market trend at that moment in time. The entropy fluctuates while tending to low values, due largely to instability in terms of the pattern of trading interactions. On the other hand, the energy increases, because in part there is a huge increase of exchange volume.

Finally, it should be noted how the combination of information provided by both the energy and entropy dimensions effectively helps to describe the detailed structure of the different crises, conveying a richer representation than if the two quantities were used singly.

In order to verify that our approach is competitive with alternatives, we have compared its performance with two well-known measurements of network structure. The first is the *Estrada index* [55] and the second the *degree assortativity coefficient* [56]. Degree assortativity represents to what extent a given node in a network relates to other nodes in the network with different degrees. The Estrada index quantifies the well-connectedness of each node. In our case, it is appropriate for comparison because it is based on the spectrum of the network adjacency matrix. In Fig. 6, we show the Estrada index and degree assortativity coefficient time series for the financial market data. Both show some evidence of fluctuation in the proximity of the market crises, but this is swamped by noise. The time series are thus difficult to interpret. For instance, for the assortativity coefficient, the so-called background looks very similar to important periods, such as the Financial Crisis of 2007–2008. As far as the Estrada index is concerned, although some relevant events seem to be better defined but are not well localized in time. Examples include the United States debt-ceiling crisis (October 2013). These comparisons suggest that our method can actually be considered a valid and more effective alternative for structural change analysis.

By changing the study modality, Fig. 7 shows the scatter plot of energy versus entropy, for the US Stock Market dataset. The main feature to note here is that different epochs of network evolution form distinct clusters, occupying different regions of the plot. In fact, the plot reveals an interesting feature of
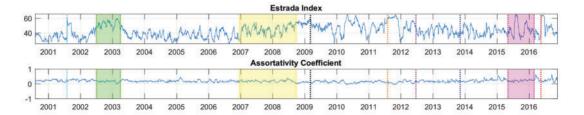
FIG. 6. USSM dataset—Estrada Index and Degree Assortativity Coefficient vs time, respectively top and bottom chart. The vertical coloured lines indicate critical events for the trade market: September 11 attacks, Downturn of 2002–2003, Financial Crisis of 2007–2008, Dow Jones lowest point (March 2009), Stock Markets Fall (August 2011), Greek legislative election (June 2012), United States debt-ceiling crisis (October 2013), Chinese stock market turbulence 2015 and Brexit Referendum (June 2016).
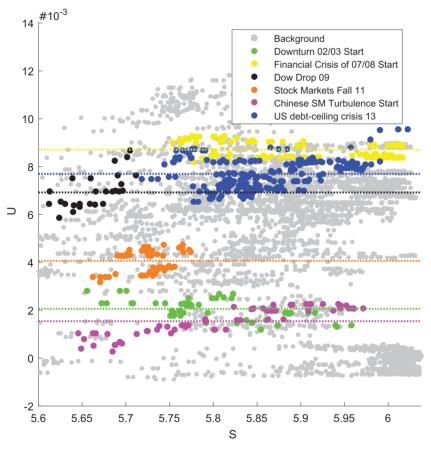

FIG. 7. USSM dataset—scatter plot of energy (U) over entropy (S). Each dot is a day and grey dots are the background. Dots of the same colour belong to the same network phase. Horizontal lines represent cluster centroids for the energy dimension.
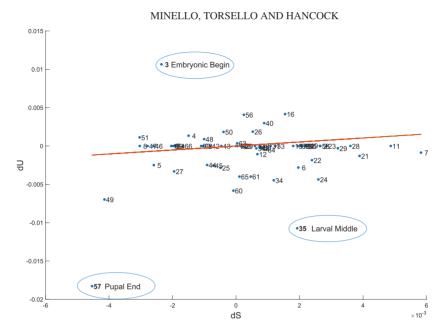
FIG. 8. *Drosophila melanogaster* dataset—scatter plot of the difference of energy vs difference of entropy, as alternative representation of the network temperature. The red line fits the trend of the temperature. Outliers are epochs when the transcript levels of the genes has changed.

the network whereby there exists a clustering tendency of the market when the system goes through strong modifications. Actually, each pattern presents a wide variation in entropy a low variation in energy. Thus, we conclude network states are better identified by energy, which effectively captures cluster compactness. Entropy on the other hand is more dispersive.

Interesting results can be observed in the experiments on the Fruit Fly data too. In Fig. 8, we show an alternative representation of the network temperature, presented as the scatter plot of the difference in energy dU over the difference in entropy dS. Most of the data clusters around a straight-line (shown in red), whose slope corresponds to the temperature of the network. However, there are also outliers exhibiting substantial departures from the main cluster. Interestingly, these samples represent fundamental developmental landmarks in the evolution of the *Drosophila melanogaster*. Specifically, they belong to the early embryonic stage, the mid-larval transaction and final stage of the pupal step. According to [35], these are three of the four major morphological changes in terms of the transcript levels of genes. In fact, they mark the beginning and end of embryogenesis, the larval–pupal transition and the end of the pupal period as shown in [35], Fig. 2A. In addition, we analyse entropy and temperature. Same as before, we performed Laplacian smoothing of the estimation of the temperature time series. In Fig. 9, the temperature (bottom time-series) clearly outperforms the entropy (top time-series), by detecting salient developmental changes during the fruit fly life cycle. Actually, entropy does not capture any information about the transcript level decline. Furthermore, by comparing the temperature dimension with the corresponding ones in [21] and [20], our method would seem to be able to capture genuine developmental stages effectively, rather than limiting the analysis to morphological changes alone.
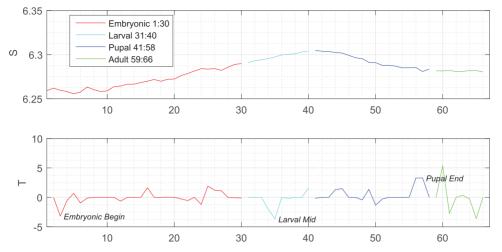
FIG. 9. *Drosophila melanogaster* dataset—entropy and temperature vs time, respectively top and bottom. The developmental periods of the fruit fly are coloured differently, and the significant moments are highlighted.

4. Non-isochoric processes

The method outlined so far was initially designed for analysing isochoric (constant volume) processes. Nevertheless, we can generalize the formulation to deal with variations in network size and, thus, in volume. We do this by assuming an isobaric process, that is, the pressure from the external environment is assumed independent of the system's evolution. By keeping a system at constant pressure, the change in volume becomes an integral part of the thermodynamic identity $dU = TdS - PdV$.

Clearly, diverse pressure levels affect the temperature differently, as the volume variation effect changes. In fact, the temperature formula can be rewritten as

$$T = \frac{dU + PdV}{dS}$$
$$= \frac{dU}{dS} + P\frac{dV}{dS}, \tag{4.1}$$

where $P\frac{dV}{dS}$ depends on the volume and pressure whereas $\frac{dU}{dS}$ depends on the energy variation.

As an implementation note, to handle density matrices with different sizes namely the dimension incongruity, we overcame the issue by padding with zeros the normalized Laplacian matrices. Then, once both the energy and the entropy variations have been recovered, we can compute the network temperature. In Fig. 10, we analyse the effect of the pressure parameter in the NYSE dataset. Here, the two temperature components are depicted simultaneously. When pressure is very small, the volume component does not contribute to the temperature. On the other hand, at high pressure values, the volume variation adds noise to the temperature. By balancing this term (in our case $P = 3 \times 10^{-5}$), the estimated temperature time-series accurately identifies occurrences of major events. In particular, the volume contribution often reinforces crucial parts of the signal, for example, during the Persian Gulf War or throughout the Russian Financial crisis, and only occasionally generates noise, for instance between the September 11 attacks and the beginning of the Downturn of 2002–2003. In fact, a comparison with [20] and [21] shows similar
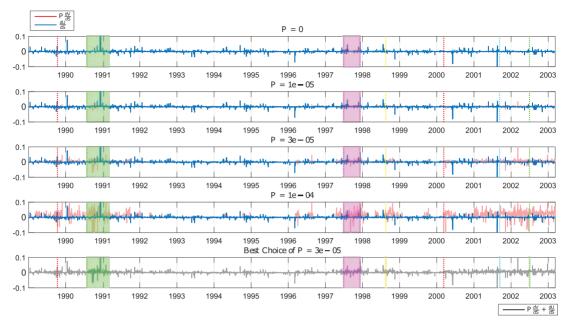
FIG. 10. NYSE dataset—temperature components vs time, as pressure changes. The vertical coloured lines indicate important events for the trade market: Friday the 13th Mini-Crash (October 1989), Persian Gulf War (August 1990–January 1991), Asian Financial Crisis (July 1997–October 1997), Russian Financial Crisis—Ruble devaluation (August 1998), Dot-com bubble—climax (March 2000), September 11 attacks and Downturn of 2002–2003.

performance in terms of event-detection accuracy, proving that the generalization to size-varying graphs is still capable of modelling the underlying dynamical processes over the networks.

5. Discussion

In this article, we have introduced a novel thermodynamic framework to characterize network structure. Specifically, our driving goal was the visualization and understanding of the evolution of the time-varying network systems. This analysis is based on quantum thermodynamics and connects to recent work on the von Neumann entropy of networks. To this end, we provided expressions for a variety of thermodynamic variables, such as entropy, energy and temperature. In particular, energy is derived by estimating an unknown Hamiltonian operator governing the free evolution of the system, that is, its evolution according the Schrödinger equation.

We have evaluated the method on real-world complex systems, from the financial and biological domains. The experimental outcomes prove that the thermodynamic state variables are effective at characterizing the evolution properties of dynamic networks, including the detection of global topological changes, phase transitions in structure or distinctive periods in the evolution of time-varying complex networks. However, we observed that the noise in the system observables or the overlap of consecutive significant events may affect the clarity of the signals, thus highlighting the level of sensitivity of the approach. Despite this, our objective of determining a correspondence between network evolution and related thermodynamic-variables has been mostly accomplished, although we are still far away from a

truly and definitive mapping between thermodynamics measures and the information provided by the system. Nevertheless, even without such a mapping, we can still indirectly obtain some useful insights. For instance, by following Ye *et al.* [21] suggestions, where entropy is seen as a measure of degree change correlations on the edges, we can infer temperature significance. Indeed, a low temperature implies a large correlation. Conversely, the greater the disruption of the pattern of correlations, the higher is the temperature.

Moreover, we were not able to identify clear precursors for the events, nor indicators of the scale of change; thus the approach as presented is mainly descriptive and, at this stage, not predictive.

There are several directions in which the work reported here can be extended. First, the work is extendable to directed graphs. In a recent article, we have reported an approximation to the von Neumann entropy of directed graphs [57], which can be used to develop a similar framework for graph in which the edges possess directionality. This may provide particularly interesting in the context of characterizing the thermodynamics of sources and sinks in a network. Second, it would be interesting to study in greater depth the manifold structure of the thermodynamic space, and understand its links to phase transitions in the structure of networks. Finally, there is the question of bidirectional entropy variation and whether this can somehow be reconciled with the second law of thermodynamics.

References

1. ANAND, K. & BIANCONI, G. (2009) Entropy measures for networks: toward an information theory of complex topologies. *Phys. Rev. E*, **80**, 045102.
2. ALBERT, R. & BARABÁSI, A.-L. (2000) Topology of evolving networks: local events and universality. *Phys. Rev. Lett.*, **85**, 5234.
3. VAN DER HOFSTAD, R. (2009) Random graphs and complex networks. Available on http://www. win. tue. nl/rhofstad/NotesRGCN. pdf, pp. 11.
4. NEWMAN, M. E.(2003) The structure and function of complex networks. *SIAM Rev.*, **45**, 167–256.
5. ESTRADA, E. (2011) *The Structure of Complex Networks: Theory and Applications*. Oxford: OUP.
6. FELDMAN, D. P. & CRUTCHFIELD, J. P. (1998) Measures of statistical complexity: why? *Phys. Lett. A*, **238**, 244–252.
7. ANAND, K., BIANCONI, G. & SEVERINI, S. (2011) Shannon and von Neumann entropy of random networks with heterogeneous expected degree. *Phys. Rev. E*, **83**, 036109.
8. MARTÍN HERNÁNDEZ, J., LI, Z. & VAN MIEGHEM, P. (2014) Weighted betweenness and algebraic connectivity. *J. Complex Netw.*, **2**, 272–287.
9. DE DOMENICO, M., NICOSIA, V., ARENAS, A. & LATORA, V. (2015) Structural reducibility of multilayer networks. *Nat. Commun.*, **6**, 6864.
10. MCCULLOH, I., & CARLEY, K. M. (2011) Detecting change in longitudinal social networks. *J. Social Struct.*, 12.
11. PEEL, L., & CLAUSET, A. (2015) Detecting change points in the large-scale structure of evolving networks. *Twenty-Ninth AAAI Conference on Artificial Intelligence*. Austin, TX: AAAI Press.
12. PRIEBE, C. E., CONROY, J. M., MARCHETTE, D. J., & PARK, Y. (2005) Scan statistics on enron graphs. *Comput. Math. Organ. Theory*, **11**, 229–247.
13. ALBERT, R. & BARABÁSI, A.-L. (2002) Statistical mechanics of complex networks. *Rev. Modern Phys.*, **74**, 47.
14. ESTRADA, E. & HATANO, N. (2007) Statistical-mechanical approach to subgraph centrality in complex networks. *Chem. Phys. Lett.*, **439**, 247–251.
15. PARK, J. & NEWMAN, M. E. (2004) Statistical mechanics of networks. *Phys. Rev. E*, **70**, 066117.
16. HUANG, K. (1987) *Statistical Mechanics*. New York: Wiley.
17. JAVARONE, M. A. & ARMANO, G. (2013) Quantum–classical transitions in complex networks. *J. Stat. Mech.*, **2013**, P04019.
18. DE DOMENICO, M., & BIAMONTE, J. (2016) Spectral entropies as information-theoretic tools for complex network comparison. *Phys. Rev. X*, **6**, 041062.

19. ESCOLANO, F., HANCOCK, E. R. & LOZANO, M. A. (2012) Heat diffusion: thermodynamic depth complexity of networks. *Phys. Rev. E*, **85**, 036206.
20. YE, C., COMIN, C. H., PERON, T. K. D., SILVA, F. N., RODRIGUES, F. A., COSTA, L. D. F., TORSELLO, A. & HANCOCK, E. R. (2015) Thermodynamic characterization of networks using graph polynomials. *Phys. Rev. E*, **92**, 032810.
21. YE, C., TORSELLO, A., WILSON, R. C. & HANCOCK, E. R. (2015) Thermodynamics of time evolving networks. *Graph-Based Representations in Pattern Recognition*. (C.-L. Liu, B. Luo, W. G. Kropatsch, J. Cheng, eds). Cham: Springer, pp. 315–324.
22. BRAUNSTEIN, S. L., GHOSH, S. & SEVERINI, S. (2006) The Laplacian of a graph as a density matrix: a basic combinatorial approach to separability of mixed states. *Ann. Combin.*, **10**, 291–317.
23. PASSERINI, F. & SEVERINI, S. (2009) Quantifying complexity in networks: the von Neumann entropy. *Int. J. Agent Technol. Syst. (IJATS)*, **1**, 58–67.
24. MIKULECKY, D. C. (2001) Network thermodynamics and complexity: a transition to relational systems theory. *Comput. & Chem.*, **25**, 369–391.
25. ESTRADA, E. & HATANO, N. (2008) Communicability in complex networks. *Phys. Rev. E*, **77**, 036111.
26. DELVENNE, J.-C. & LIBERT, A.-S. (2011) Centrality measures and thermodynamic formalism for complex networks. *Phys. Rev. E*, **83**, 046117.
27. BIANCONI, G. & BARABÁSI, A.-L. (2001) Bose–Einstein condensation in complex networks. *Phys. Rev. Lett.*, **86**, 5632.
28. CHUNG, F. R. (1997) *Spectral Graph Theory*, vol. 92. Providence, RI: American Mathematical Society.
29. WANG, J., WILSON, R. C. & HANCOCK, E. R. (2016) Network entropy analysis using the Maxwell-Boltzmann partition function. *2016 23rd International Conference on Pattern Recognition (ICPR)*. (L. Davis, B. A. Del and B. Lovell, eds). Los Alamitos, CA: IEEE, pp. 1321–1326.
30. WANG, J., WILSON, R. C. & HANCOCK, E. R. (2017) Spin statistics, partition functions and network entropy. *J. Complex Netw.*, **5**, 858–883.
31. WANG, J., WILSON, R. C. & HANCOCK, E. R. (2016b) Thermodynamic network analysis with quantum spin statistics. *Joint IAPR International Workshops on Statistical Techniques in Pattern Recognition (SPR) and Structural and Syntactic Pattern Recognition (SSPR)*. (A. Robles-Kelly, M. Loog, B. Biggio, F. Escolano, R. Wilson, eds). Cham: Springer, pp. 153–162.
32. WANG, J., WILSON, R. C. & HANCOCK, E. R. (2017a) Minimising entropy changes in dynamic network evolution. *International Workshop on Graph-Based Representations in Pattern Recognition*. (P. Foggia, C.L. Liu, M. Vento, eds): Cham: Springer, pp. 255–265.
33. ZUREK, W. H. (1993) Preferred states, predictability, classicality and the environment-induced decoherence. *Prog. Theor. Phys.*, **89**, 281–312.
34. PERON, T. D. & RODRIGUES, F. A. (2011) Collective behavior in financial markets. *EPL (Europhys. Lett.)*, **96**, 48004.
35. ARBEITMAN, M. N., FURLONG, E. E., IMAM, F., JOHNSON, E., NULL, B. H., BAKER, B. S., KRASNOW, M. A., SCOTT, M. P., DAVIS, R. W. & WHITE, K. P. (2002) Gene expression during the life cycle of *Drosophila melanogaster. Science*, **297**, 2270–2275.
36. SONG, L., KOLAR, M. & XING, E. P. (2009) KELLER: estimating time-varying interactions between genes. *Bioinformatics*, **25**, i128–i136.
37. BRIEGEL, H. J. & RAUSSENDORF, R. (2001) Persistent entanglement in arrays of interacting particles. *Phys. Rev. Lett.*, **86**, 910.
38. HEIN, M., EISERT, J. & BRIEGEL, H. J. (2004) Multiparty entanglement in graph states. *Phys. Rev. A*, **69**, 062311.
39. BLINOV, B., MOEHRING, D., DUAN, L.-M. & MONROE, C. (2004) Observation of entanglement between a single trapped atom and a single photon. *Nature*, **428**, 153.
40. BOSE, S. (2007) Quantum communication through spin chain dynamics: an introductory overview. *Contemp. Phys.*, **48**, 13–30.
41. KIELPINSKI, D., MONROE, C. & WINELAND, D. J. (2002) Architecture for a large-scale ion-trap quantum computer. *Nature*, **417**, 709–711.

42. HILDEBRAND, R., MANCINI, S. & SEVERINI, S. (2008) Combinatorial Laplacians and positivity under partial transpose. *Math. Struct. Comput. Sci.*, **18**, 205–219.

43. DE BEAUDRAP, N., GIOVANNETTI, V., SEVERINI, S. & WILSON, R. (2016) Interpreting the von Neumann entropy of graph Laplacians, and coentropic graphs. *A Panorama of Mathematics: Pure and Applied*, vol. 658, pp. 227.

44. NIELSEN, M. & CHUANG, I. (2010) *Quantum Computation and Quantum Information*. Cambridge: Cambridge University Press.

45. DAIRYKO, M., HOGBEN, L., LIN, J. C.-H., LOCKHART, J., ROBERSON, D., SEVERINI, S. & YOUNG, M. (2017) Note on von Neumann and Rényi entropies of a graph. *Linear Algebra Appl.*, **521**, 240–253.

46. DU, W., LI, X., LI, Y. & SEVERINI, S. (2010) A note on the von Neumann entropy of random graphs. *Linear Algebra Appl.*, **433**, 1722–1725.

47. SIMMONS, D. E., COON, J. P. & DATTA, A. (2018) The von Neumann Theil index: characterizing graph centralization using the von Neumann index. *J. Complex Netw.*, **6**, 859–876.

48. MINELLO, G., ROSSI, L. & TORSELLO, A. (2019) On the von Neumann entropy of graphs. *J. Complex Netw.*, **7**, 491–514.

49. ROSSI, L., TORSELLO, A., HANCOCK, E. R. & WILSON, R. C. (2013) Characterizing graph symmetries through quantum Jensen-Shannon divergence. *Phys. Rev. E*, **88**, 032806.

50. FARHI, E. & GUTMANN, S. (1998) Quantum computation and decision trees. *Phys. Rev A*, **58**, 915.

51. MAGNUS, W. (1954) On the exponential solution of differential equations for a linear operator. *Commun. Pure Appl. Math.*, **7**, 649–673.

52. HAUSDORFF, F. (1906) Die symbolische Exponentialformel in der Gruppentheorier. *Ber. Verh. Kgl. SÃ chs. Ges. Wiss. Leipzig., Math.-phys. Kl.*, **58**, 19–48.

53. CANTWELL, G. T., LIU, Y., MAIER, B. F., SCHWARZE, A. C., SERVÁN, C. A., SNYDER, J. & ST-ONGE, G. (2019) Thresholding normally distributed data creates complex networks. ArXiv, abs/1902.08278.

54. BRAUNSTEIN, S. L., GHOSH, S., MANSOUR, T., SEVERINI, S. & WILSON, R. C. (2006) Some families of density matrices for which separability is easily tested. *Phys. Rev. A*, **73**, 012320.

55. ESTRADA, E. (2000) Characterization of 3D molecular structure. *Chem. Phys. Lett.*, **319**, 713–718.

56. NEWMAN, M. E. (2002) Assortative mixing in networks. *Phys. Rev. Lett.*, **89**, 208701.

57. YE, C., WILSON, R. C., COMIN, C. H., COSTA, L. D. F. & HANCOCK, E. R. (2014) Approximate von Neumann entropy for directed graphs. *Phys. Rev. E*, **89**, 052804.